Table II. Hearing profiles and MRI auditory pathway myelination in PMD patients.

Parameter	Patient 1		Patient 2		Patient 3		Patient 4		Patient 5		Patient 6		Patient 7		Patient 8	
Hearing profile	Left	Right	Left	Right	Left	Right	Left	Right	Left	Right	Left	Right	Left	Right	Left	Right
Audiometry (last visit)	27 dB	27 dB	37.5 dB	37.6 dB	35 dB	36 dB	18.8 dB	17.5 dB	39 dB	39 dB	35 dB	35 dB	3.3 dB	5 dB	36 dB	36 dB
DPOAE	NA	NA	NA	NA	Normal	Normal	Normal	Normal	Normal	Normal	Normal	Normal	Normal	Normal	Normal	Normal
ABR																
Wave I	Prolonged	Prolonged	Prolonged	Prolonged	Prolonged	Prolonged	Prolonged	Prolonged	–	–	–	–	–	–	–	–
Wave II	Prolonged	Prolonged	Prolonged	Prolonged	Prolonged	Prolonged	–	–	–	–	–	–	–	–	–	–
Wave III	–	–	–	–	–	–	–	–	–	–	–	–	–	–	–	–
Wave IV	–	–	–	–	–	–	–	–	–	–	–	–	–	–	–	–
Wave V	–	–	–	–	–	–	–	–	–	–	–	–	–	–	–	–
MRI findings																
Scan age	2 years 6 months		1 year		1 year 6 months		2 years	10 months	2 years 6 months		5 years		17 years		7 months	
Morphological abnormalities																
Cerebrum atrophy	Normal		Normal		Normal		Normal	Normal	Normal		Normal		Normal		Normal	
Cerebellum atrophy	Normal		Normal		Normal		Normal	Normal	Normal		Normal		Normal		Normal	
Tigroid appearance	Cetrum semiovale		Cetrum semiovale		Cetrum semiovale		Cetrum semiovale	Cetrum semiovale	Cetrum semiovale		Cetrum semiovale		Cetrum semiovale		Cetrum semiovale	
Auditory radiation	–		–		–		–	–	–		–		–		–	
Medial geniculate body	+/–		–								–				–	
Inferior colliculus																
branchium																
Lateral lemniscus																
Superior olive																
Cochlear nucleus			NA												NA	
Cochlear nerve																

+, indicates myelinated regions, defined as hypointensity on T2-weighted images; –, indicates nonmyelinated regions, defined as hyperintensity on T2-weighted images; +/–, indicates transition between the two values. Dark gray shading indicates regions showing hypointensity on T2-weighted images, thus indicating myelinated regions; light gray shading indicates incomplete or partial myelination. NA, not available for evaluation.

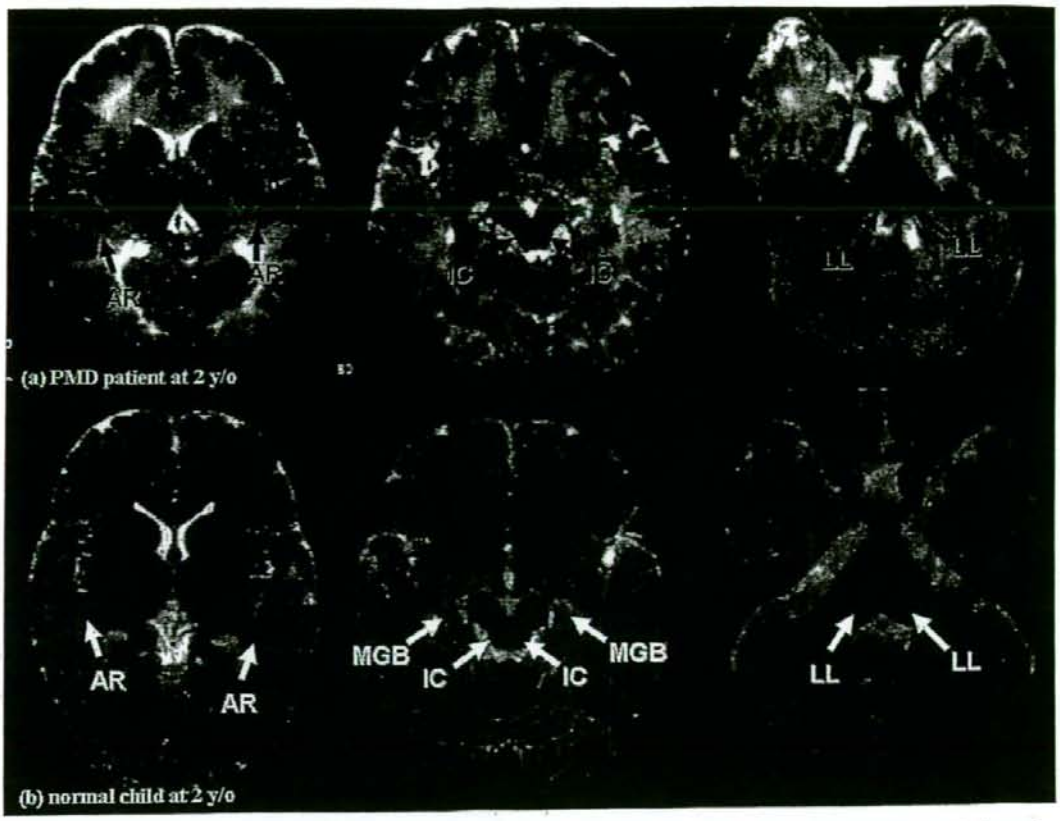

Figure 2. (a) The upper row shows that T2-weighted magnetic resonance imaging (MRI) results of patient 3 at age 2 resemble those of a normal neonate, suggesting that the arrest of myelination occurs soon after birth in PMD. (b) The lower row shows the normal myelination of a young child at age 2. Myelination process reached the auditory radiation. AR, auditory radiation; MGB, medial geniculate body; IC, inferior colliculus brachium; LL, lateral lemniscus.

of the degree of hearing impairment, all the patients showed delayed auditory myelination. Myelination only reached the inferior colliculus brachium or medial geniculate body; it did not reach the auditory radiation. There seems to be no clear relation between hearing threshold and myelination milestones. Also,

Table III. MRI auditory pathway myelination in normal young children (control group).

MRI findings								
Scan age	0 months	3 months	6 months	9 months	1 year	1 year 3 months	1 year 6 months	2 years
Number of subjects	3	3	3	3	4	3	2	2
Auditory pathway myelination								
Auditory radiation	–	–	–	–	+/–			
Medial geniculate body	+/–							
Inferior colliculus brachium	+/–							
Lateral lemniscus	+/–							
Superior olive								
Cochlear nucleus								
Cochlear nerve								

+, indicates myelinated regions, defined as hypointensity on T2-weighted images; –, indicates nonmyelinated regions, defined as hyperintensity on T2-weighted images; +/–, indicates transition between the two values. Dark gray shading indicates regions showing hypointensity on T2-weighted images, thus indicating myelinated regions; light gray shading indicates incomplete or partial myelination. NA, not available for evaluation.

no relation was found between ABR findings and MRI-assessed myelination of the auditory pathway. By comparing the MRI results in PMD patients with the normal myelination milestones in the control group, we found that the myelination process of the auditory pathway in PMD seemed to cease between the ages of 0 and 6 months, was limited to the brainstem, and left the cerebral white matter unmyelinated. The second MRI scan in one patient also showed the absence of any progression in myelination. This is consistent with previous studies showing that an arrest of myelination occurs before or soon after birth in PMD [3,4,21–23]. Some reports, particularly in female cases, showed that myelination was slowly improving parallel to the ABR findings [20]. In our studies, we are unable to confirm whether the myelination is arrested or still progressing in the auditory pathway, since MRI was carried out only once on seven of the eight subjects and twice on one subject. Also the young as well as older subjects show lack of myelination irrespective of age.

Neuropathologically, PMD has been characterized by the lack of myelination in the central nervous system. In the classical form of PMD, patchy myelin deficits were observed in the cerebral white matter, particularly in the centrum semiovale. These preserved myelin islets have no association with neuroanatomical structures, such as fiber pathways and systems, but are frequently found perivascularly, sometimes as zones of preserved myelin along stretches of blood vessels, thus giving rise to the characteristic tigroid appearance [2–5]. The cerebellar white matter was less seriously affected, although it still showed the tigroid appearance. The brainstem and spinal cord showed almost normal myelination or sometimes only modest and focal decrease in the staining intensity of myelinated fibers. Cranial nerves, spinal roots, and peripheral nerves are normally myelinated [2,4,5,23,24]. However, toHhe connatal form of PMD is characterized by the total lack of myelination in the cerebrum, cerebellum, and brainstem, with the spinal roots and cranial nerves being normally myelinated [4,5,23–25]. Our MRI results are consistent with the pathological findings of classic PMD; however, to our knowledge there have been no pathologic descriptions of the auditory pathway of PMD in previous studies.

This raises the question of how patients with PMD perceive sound stimuli because they lack myelination past the inferior colliculus or medial geniculate body in the auditory pathway. We postulate that axons in the auditory pathway are sufficiently preserved to conduct the sound stimulus even though myelin is essentially absent in the subcortical white matter. These observations are compatible with those of the visual pathway in PMD patients in previous studies. Those patients retained pupillary light reflexes despite visual impairment and optic atrophy. The interpretation was that axons in the optic nerves are sufficiently preserved to conduct the light stimulus even though myelin is essentially absent [24]. Moreover, previous histological studies of the classic form of PMD showed a nearly normal axon density and a normal number of nerve cells in the brainstem and a mildly reduced number of axons and nerve cells in the affected subcortical white matter [4,5,23,24].

In this study, we demonstrated that delayed auditory pathway myelination is common in PMD, but it does not necessarily indicate poor hearing function. The serial audiometry suggested that hearing threshold improves over time. The ABR showed absence of later waves, which may indicate some asynchrony of firing at brainstem level. However, MRI does not show abnormal patterns in the corresponding structures of the brainstem. We may conclude that MRI does not show the same aspects of neural function as ABR and hearing threshold. Further studies should be conducted to clarify the pathogenesis and observe the long-term prognosis of hearing function in this disease. Finally, despite the rarity of PMD, the PLP mutations in humans and animals have generated enormous interest due to their importance for our understanding of myelination and myelin repair.

References

[1] Pelizaeus F. Ueber eine eigenthumliche Form spastischer Lähmung mit Cerebralerscheinungen auf hereditärer Grundlage (Multiple Sklerose). Arch Psychiat Nervenkrankh 1885;16:698–710.

[2] Merzbacher L. Eine eigenartige familiär-hereditäre Erkrankungsform (Aplasia axialis extracorticalis congenita). Zeitschr Ges Neurol Psychiat 1910;3:1–138.

[3] Koeppen AH, Ronca NA, Greenfield EA, Hans MB. Defective biosynthesis of proteolipid protein in Pelizaeus-Merzbacher disease. Ann Neurol 1987;21:159–70.

[4] Seitelberger F. Pelizaeus-Merzbacher disease. In: Vinken PJ, Bruyn GW, editors. Handbook of clinical neurology, vol 10 (Leucodystrophies and poliodystrophies). Amsterdam: North-Holland; 1970. p. 150–202.

[5] Seitelberger F. Neuropathology and genetics of Pelizaeus-Merzbacher disease. Brain Pathol 1995;5:267–73.

[6] Tranebjaerg L, Schwartz C, Eriksen H. A new X linked recessive deafness syndrome with blindness, dystonia, fractures, and mental deficiency is linked to Xq22. J Med Genet 1995;32:257–63.

[7] Seeman P, Paderova K, Benes V Jr. A severe connatal form of Pelizaeus Merzbacher disease in a Czech boy caused by a novel mutation (725C>A, Ala242Glu) at the 'jimpy(msd) codon' in the PLP gene. Int J Mol Med 2002;9:125–9.

[8] Battini R, Bianchi MC, Boespflug-Tanguy O, Tosetti M, Bonanni P, Canapicchi R. Unusual clinical and magnetic resonance imaging findings in a family with proteolipid protein gene mutation. Arch Neurol 2003;60:268–72.

[9] Bonavita S, Schiffman R, Moore DF, Frei K, Choi B, Patronas MD, et al. Evidence of neuroaxonal injury in

patients with proteolipid protein gene mutations. Neurology 2001;56:785–8.
[10] Nezu A. Neurophysiological study in Pelizaeus-Merzbacher disease. Brain Dev 1995;17:175–81.
[11] Kaga K, Tamai F, Kodama M, Kodama K. Three young adult patients with Pelizaeus-Merzbacher disease who showed only waves I and II in auditory brainstem responses but had good auditory perception. Acta Otolaryngol (Stockh) 2005;125:1018–23.
[12] Kaga K, Yokochi K, Kitazumi E. Absence of later auditory brain stem response components, congenital horizontal nystagmus, and hypotonia in male infants. Ann Otol Rhinol Laryngol 1986;95:203–6.
[13] Bird CR, Hedberg M, Drayer BP, Keller PJ, Flom RA, Hodak JA. MR assessment of myelination in infants and children: usefulness of marker sites. AJNR Am J Neuroradiol 1989;10:731–40.
[14] van der Knaap MS, Valk J, Bakker CJ, Schooneveld M, Faber JA, Willemse J, et al. Myelination as an expression of the functional maturity of the brain. Dev Med Child Neurol 1991;33:849–57.
[15] Konishi Y, Hayakawa K, Kuriyama M, Fujii Y, Sudo M, Konishi K, et al. Developmental features of the brain in preterm and fullterm infants on MR imaging. Early Hum Dev 1993;34:155–62.
[16] Barkovich AJ, Kjos BO, Jackson DE Jr, Norman D. Normal maturation of the neonatal and infant brain: MR imaging at 1.5 T. Radiology 1988;166:173–80.
[17] Counsell SJ, Rutherford MA. Magnetic resonance imaging of the newborn brain. Current Paediatrics 2002;12:401–13.
[18] Barkovich AJ. MR of the normal neonatal brain: assessment of deep structures. AJNR Am J Neuroradiol 1998;19:397–403.
[19] Henkel CK. The auditory system. In: Haines DE, editor. Fundamental neuroscience. Pennsylvania: Churchill Livingstone; 2002. p. 323–40.
[20] Inoue K, Tanaka H, Scaglia F. Compensating for central nervous system dysmyelination: females with a proteolipid protein gene duplication and sustained clinical improvement. Ann Neurol 2001;50:747–54.
[21] Nezu A, Kimura S, Takeshita S, Osaka H, Kimura K, Inoue K. An MRI and MRS study of Pelizaeus-Merzbacher disease. Pediatr Neurol 1998;18:334–7.
[22] van der Knaap MJ, Valk J. Myelin and white matter. In: van der Knaap MJ, Valk J, editors. Magnetic resonance of myelin, myelination, and myelin disorders, 2nd edn. Berlin: Springer; 1995. p. 1–17.
[23] Sasaki A, Miyanaga K, Ototsuji M, Iwaki A, Iwaki T, Takahashi S, et al. Two autopsy cases with Pelizaeus-Merzbacher disease phenotype of adult onset, without mutation of proteolipid protein gene. Acta Neuropathol 2000;99:7–13.
[24] Seitelberger F. Neuropathology and genetics of Pelizaeus-Merzbacher disease. Brain Pathol 1995;5:267–73.
[25] Koeppen A, Robitaille Y. Pelizaeus-Merzbacher disease. J Neuropathol Exp Neurol 2002;61:747–59.

International Journal of Pediatric Otorhinolaryngology (2008) 72, 1479–1486

ELSEVIER

International Journal of Pediatric Otorhinolaryngology

www.elsevier.com/locate/ijporl

Early myelination patterns in the central auditory pathway of the higher brain: MRI evaluation study

Masaki Sano [a,*], Chen-Chieh Kuan [a], Kimitaka Kaga [a], Kenji Itoh [b], Kenji Ino [c], Kazuo Mima [c]

[a] *Department of Otorhinolaryngology and Head & Neck Surgery, Graduate School of Medicine and Faculty of Medicine, University of Tokyo, 7-3-1 Hongo, Bunkyo-ku, Tokyo 113-8655, Japan*
[b] *Department of Cognitive Neuroscience, Graduate School of Medicine and Faculty of Medicine, University of Tokyo, Tokyo, Japan*
[c] *Division of Radiology, University of Tokyo Hospital, Tokyo, Japan*

Received 7 March 2008; received in revised form 14 June 2008; accepted 18 June 2008
Available online 3 August 2008

KEYWORDS
Myelination;
MRI study;
Medial geniculate body;
Auditory radiation;
Splenium of the corpus callosum

Summary

Objective: The purpose of this study was to use magnetic resonance imaging (MRI) to investigate the early myelination patterns of the central auditory pathway and then compare the data with past histological research. We observe the MRI signal intensity of the central auditory pathway and clarify the time course difference between MRI and previous histological research studies.
Methods: A total of 192 infants ranging in age from −4 to 224 corrected postnatal weeks were included in the study. Images were obtained using a 1.5 T MR unit. We chose three sites (medial geniculate body, auditory radiation, and splenium of the corpus callosum) of the central auditory pathway for analysis. Three cross sections were obtained perpendicular to the long axis of the brain and used to analyze the signal changes of the T1- and T2-weighted MRI by employing a region-of-interest (ROI) methodology that was corrected for postnatal age.
Results: At 10 corrected postnatal weeks, the medial geniculate body showed myelinated intensity changes on T2-weighted images. Auditory radiation showed myelinated intensity changes at 19 corrected postnatal weeks on the T1-weighted images and at 24 corrected postnatal weeks on the T2-weighted images. The splenium of the corpus callosum showed myelinated intensity changes at 16 corrected postnatal weeks on T1-weighted images and at 24 corrected postnatal weeks on T2-weighted images.
Conclusions: As compared to the histological literature, the MRI documented signal intensity changes caused by myelination occurred approximately 3 weeks later for the medial geniculate body, 7–24 weeks later for the auditory radiation and 7–15 weeks later for the splenium of the corpus callosum. Since myelination is a process that occurs

* Corresponding author. Tel.: +81 3 5800 8665; fax: +81 3 3814 9486.
E-mail address: neurootolsano@ybb.ne.jp (M. Sano).

0165-5876/$ – see front matter
doi:10.1016/j.ijporl.2008.06.011

gradually, substantial changes of the myelin sheath makeup, a loss of water and the addition of lipids are more required in order to be detectable by MRI than myelin staining of histological study.

1. Introduction

We have previously reported the early myelination patterns of the brainstem auditory pathway using MRI and clarified the time course difference that has been reported to occur between MRI and histological research data [1]. In the current study, we attempted the same study for the central auditory pathway of the higher brain. The higher brain structures of the central auditory pathway are the medial geniculate body, auditory radiation and splenium of the corpus callosum. Histologically, the degree of myelination in the central auditory pathway of the higher brain has been studied from the viewpoint that it is a maturation parameter of the auditory system during early childhood [2–5]. In 1920, Flechsig [2] reported that myelination occurred at 7 weeks in the medial geniculate body, and at 9 weeks in both the auditory radiation and splenium of the corpus callosum. As reported by Yakovlev and Lecours [3] the auditory radiation exhibited myelination at 0 weeks while there was myelination at 16 week in the splenium of the corpus callosum. MRI signal intensity changes provide considerably more information about the myelination process than other methodologies, [6–16] and thus, MRI is quite useful when attempting to evaluate central nervous system myelination. During the progress of myelination, MRI signal intensities change from low to high for the T1-weighted imaging, and from high to low for the T2-weighted imaging [17–20]. Therefore, we used MRI to investigate the signal intensity of the central auditory pathway in infants as they age and then compared our results with previous histological research studies.

2. Patients and methods

2.1. Patients

Among subjects who underwent brain MRIs between 2000 and 2005 at the University of Tokyo Hospital, we examined a total of 192 neonates, infants and small children (98 males, 94 females), with a mean age of 8.7 weeks (range, −4 to 224 corrected postnatal weeks, with minus weeks indicating a premature infant (Fig. 1). Subjects were examined by MRI due to suspicion of a brain disorder and asphyxia, hyperbilirubinemia, low birth weight, muscular dystrophy, epilepsy, mental retardation, chromosome aberration, spasm, head injury. And anomalies, infarcts, or hemorrhages and brain lesions or severe central nervous system malformations in the central auditory pathway, myelination disorder pointed out by the radiologist were excluded from the study. Deaf children that became clearly by following inspection were also excluded.

2.2. Imaging methods

Imaging was performed using 1.5 T MR units (Magnetom Vision 1.5 T, Siemens, Germany; Signa Excite HD 1.5 T, GE, USA). T1-weighted images were obtained using spin-echo or inversion recovery sequences and T2-weighted images were obtained using spin-echo sequences. All sections were perpendicular to the long axis of the brain and were 5–7 mm thick. Repetition time (TR) was 300–600 ms in the T1-weighted images and 3000 ms in the T2-weighted images. Echo time (TE) was 10–20 ms in the T1-weighted images and 70–100 ms in the T2-weighted images.

2.3. Evaluation methods

MRI has been reported to be useful for evaluating myelination in the central nervous system [6]. With MRI, it is possible to observe the internal structures of the brain [21]. When there are changes in the signal intensity associated with myelination on T1- and T2-weighted images, these changes are indicative of the lipid and water content changes that accompany the developing myelin [8,22]. For the T1-weighted imaging, the signal intensity progresses from hypo- to hyperintensity when myelination occurs and becomes distinguishable as a hyperintense area. With T2-weighted imaging, the signal intensity progresses from hyper- to hypointensity when myelination occurs and becomes distinguishable as a hypointense area [16–18]. However, as the surrounding tissue develops and begins to display similar signal intensities to those seen for the nucleus or tracts (continued progress of the myelination in the surrounding white or gray matter), they become difficult to distinguish from the surrounding tissue on MRI, which is a phenomenon referred to as blurring [6].

For the present study, 1152 MRI images were examined (192 cases, 6 slices by T1- and T2-

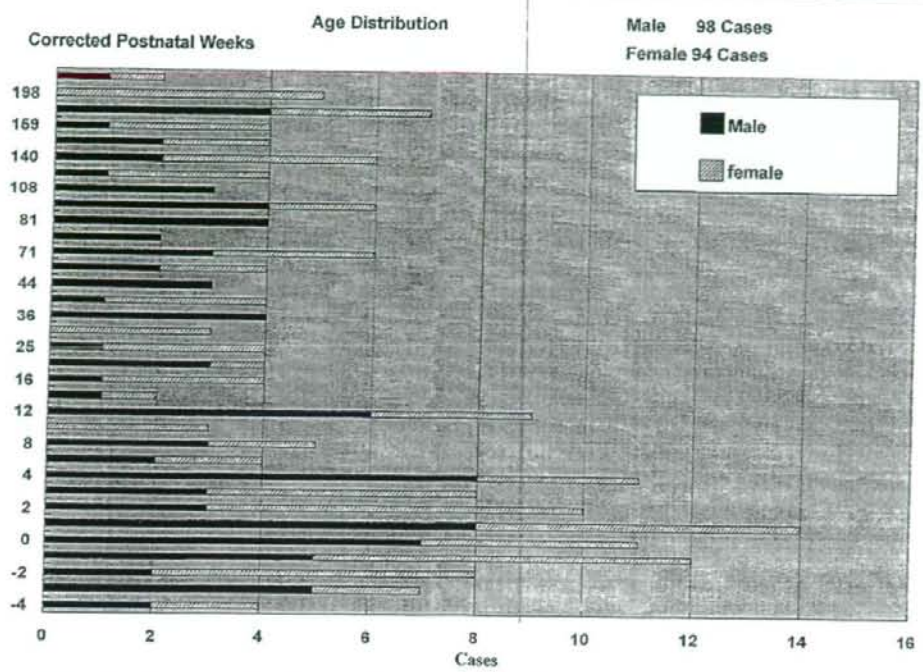

Fig. 1 Histogram shows the age distribution of MRI. We examined a total of 192 neonates, infants and small children (98 males, 94 females), with a mean age of 8.7 weeks (range, −4 to 224 corrected postnatal weeks, with minus weeks indicating a premature infant.

weighted imaging). We analyzed the myelination progress patterns at three different points (medial geniculate body, auditory radiation, and splenium of the corpus callosum) in accordance with a region-of-interest (ROI)-based analysis.

2.4. Depiction of ROIs (Fig. 2)

ROIs were located in the central auditory pathway and in the areas that surrounded each point of interest. The identification of the structure was confirmed by consulting a fetal neuroanatomy textbook [23] along with data from a previous study on term neonates [15]. Fig. 2(1) indicates the medial geniculate body (arrow) and the surrounding white matter (arrowhead) in a slice of the brainstem taken at the thalamus. Fig. 2(2) indicates the auditory radiation (arrow) and the surrounding white matter (arrowhead). Fig. 2(3) indicates the splenium of the corpus callosum (arrow) and the surrounding gray matter (arrowhead).

2.5. ROI-based analysis

Counts for each ROI were measured using Centricity Web-J software (GE Yokogawa Medical System Co. Ltd., Tachikawa, Japan). Signal intensity ratio (SIR) was defined as a difference noted between the ROI value at each assessment site of the central auditory pathway and the corresponding surrounding tissue.

SIR was calculated as follows: (ROI value of assessment site − the ROI value of surrounding tissue/ROI value of the assessment site) × 100. For example, if the ROI value of the medial geniculate body was 1000 and the ROI value of surrounding tissue was 800, SIR = (1000 − 800/1000) × 100 = 20. The SIR value of both sides was measured for each evaluation part, with the average value then computed.

2.6. Statistical analysis

We analyzed SIR in relation to corrected postnatal weeks. Corrected postnatal weeks (CPW) are required when working with premature born infants. The adjustment is calculated by subtracting the number of months that the child was born prematurely from the current age. For example, if a child is born at 28 gestational weeks (3 months before due date), the imaging done at the age of 9 months should yield values consistent with a 6-month-old child (9 minus 3). Corrected postnatal weeks were calculated according to the definition set by the University of Washington (UW)'s home-

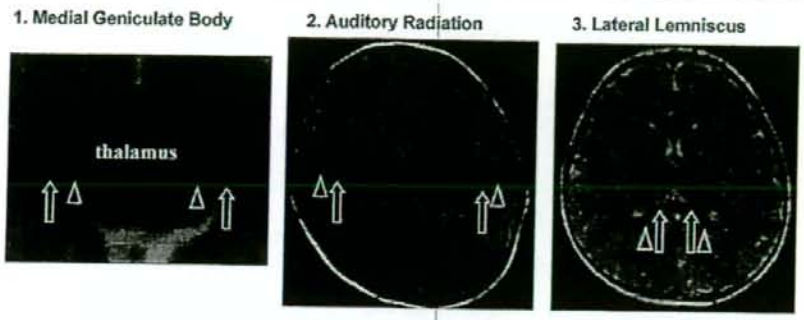

Fig. 2 Depiction of ROIs (T2-weighted images). Arrow indicates each point of the central auditory pathway (medial geniculate body, auditory radiation and splenium of the corpus callosum), with arrowhead indicating the surrounding gray or white matter. The identification of the structure was confirmed by consulting a fetal neuroanatomy textbook along with data from a previous study on term neonates. (1) Medial geniculate body (arrow) and surrounding white matter (arrowhead). (2) Auditory radiation (arrow) and surrounding gray matter (arrowhead). (3) Splenium of the corpus callosum (arrow) and surrounding gray matter (arrowhead). After pointing these structures we did region-of-interest (ROI)-based analysis using Centricity Web-J software (GE Yokogawa Medical System Co. Ltd., Tachikawa, Japan).

page entitled, "Gaining and growing: Calculating corrected age [24].

SIR was calculated for each of the images as previously discussed in the above ROI-based analysis section, with SPSS ver. 14.0 software for Windows (SPSS 14.0 Japan) used for the analyses. Using Excel for Windows (Microsoft, USA), mean SIR was calculated using the same corrected postnatal weeks (CPW), with the number of postnatal weeks plotted on the *X*-axis and SIR plotted on the *Y*-axis. For the T1-weighted imaging, positive high SIR values are indicative of myelination, while for T2-weighted imaging, negative low SIR values are indicative of myelination. A lower SIR for the T1-weighted imaging and a higher SIR for the T2-weighted imaging after the myelination period indicates the occurrence of blurring.

Subsequently, we then determined the number of weeks for which the comparison of the average value for each section exhibited a significant difference when using Sigma Stat for Windows software version 3.5 (Systat Software, CA, USA). One-way factorial ANOVA was used to investigate the difference between the average SIR values among each section, followed by Bonferroni's multiple comparison tests for mutual comparison. A p-value less than 0.05 denoted the presence of a significant difference.

3. Results

The medial geniculate body, which includes the gray matter nuclei, did not exhibit any significant differences throughout all of the CPW for the T1-weighted imaging ($p > 0.05$). However, significant differences were observed between the <10 CPW and the 10–48 CPW cases. Additionally, significant differences were noted between the 10–48 CPW and the >48 CPW cases for the T2-weighted imaging ($p < 0.05$) (Fig. 3).

The auditory radiation, which includes the white matter tract, displayed significant differences between the <19 CPW and the >19 CPW cases ($p < 0.05$). There were significant differences noted in the T2-weighted images between the <24 CPW and the >24 CPW cases ($p < 0.05$) (Fig. 4).

The splenium of the corpus callosum, which is a white matter tract, displayed significant differences between the <16 CPW and >16 CPW cases for the T1-weighted imaging ($p < 0.05$). For the T2-weighted images, significant differences were noted between the <24 CPW and >24 CPW cases ($p < 0.05$) (Fig. 5).

4. Discussion

4.1. MRI study of myelination and compare with histological study

Numerous research groups [6,8,12–15,20,25–27] have used MRI to document central nervous system changes corresponding to myelination in the developing neonate and infant. However, most of these radiological reports did not examine or report data on the central auditory pathway. In some studies that did examine one part of the central auditory pathway (Table 1), Counsell et al. [28] used 1.0 T MRI to analyze the medial geniculate body in 26 preterm infants with a median fetal age of 28 weeks. They examined myelination-associated T2-weighted

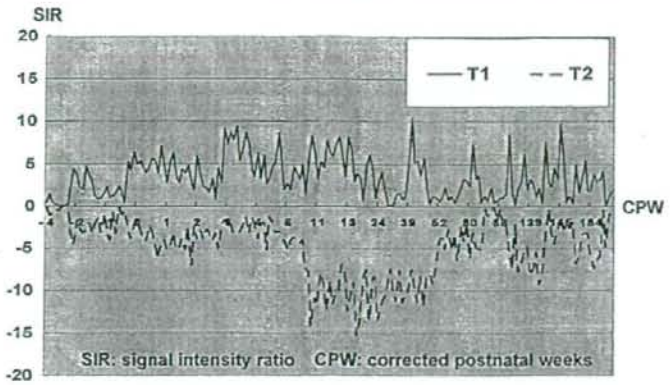

Fig. 3 SIR changes for the medial geniculate body (T1 and T2 weighted) SIR was calculated as follows: (ROI value of assessment site − the ROI value of surrounding tissue/ROI value of the assessment site) × 100. The SIR value of both sides was measured for each evaluation part, with the average value then computed. *X*-axis: corrected postnatal weeks (CPW), *Y*-axis: signal intensity ratio (SIR).

signal changes and determined that the medial geniculate body exhibited signal changes that were indicative of myelination at 28 fetal weeks (fw), which is much earlier than what we found in the current study. Nakagawa et al. [6] used 1.5 T MRI to examine the auditory radiation and splenium of the corpus callosum and found signal changes for both areas at 54–67 gestational weeks (both T1- and T2-weighted). After converting gestational weeks to weeks after birth (gestational weeks minus 40 weeks), their results were similar to our results. Bird et al. [16] examined the splenium of the corpus callosum and reported finding myelination at 10 months of age (40 weeks after birth). The difference between their results and the findings of our study most likely originate from methodological differences, as a visual evaluation by the researchers was used by Counsell et al. [28], Nakagawa et al. [6] and Bird et al. [16], while objective ROI measurements were employed in this study.

In our MRI study, the medial geniculate body, which contains the gray matter nuclei, started to show changes in the myelination signal at 10 CPW, with blurring occurring at 48 CPW on T2-weighted imaging. Even though the MRI can detect myelination signal intensity changes in the medial geniculate body, once blurring occurs, myelination signal intensity is no longer detectable. Blurring phenomenon which became difficult to distinguish central nucleus or pathway from the surrounding tissue on MRI is reported by Nakagawa et al. [6] as well as our study. A proposed theory for why this "blurring" phenomenon occurs can be explained from research of Moore et al. [5]. Moore's histological report compared material from adults and fetuses, they noted in adults, the myelinated axons fill the surrounding

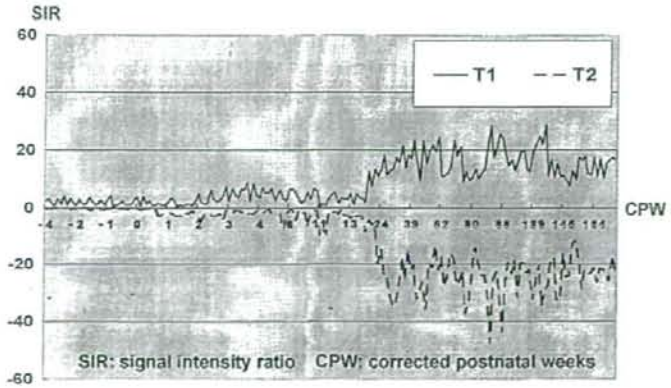

Fig. 4 SIR changes for the auditory radiation (T1 and T2 weighted). *X*-axis: corrected postnatal weeks (CPW), *Y*-axis: signal intensity ratio (SIR).

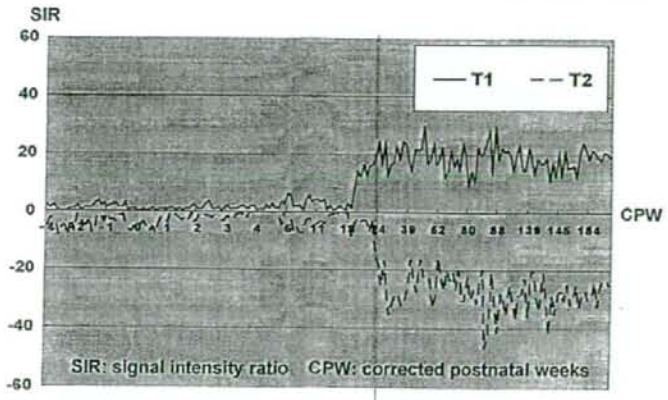

Fig. 5 SIR changes for the splenium of the corpus callosum (T1 and T2 weighted). *X*-axis: corrected postnatal weeks (CPW), *Y*-axis: signal intensity ratio (SIR).

tissue of central nervous nucleus (this means that MRI signal intensity of surrounding tissue changes as same as central nervous nucleus = blurring), so it become less prominent in adults as compared to that seen during the fetal period which shows contrast of central nervous nucleus and surrounding tissue. In our study we noted that the auditory radiation, which is a white matter tract, exhibited myelination-associated signal changes at 19 CPW at which point no blurring had occurred on the T1-weighted imaging. For the T2-weighted imaging, myelination- associated signal changes occurred at 24 CPW at which time there was also no blurring noted. The splenium of the corpus callosum, which is a white matter tract, showed myelination-associated signal changes at 16 and 24 CPW on the T1- and T2-weighted imaging, respectively. In both cases, no blurring was observed. Auditory radiation and the splenium of the corpus callosum are large structure of white matter tracts, it was considered that blurring phenomenon does not observed.

Flechsig's original results [2] documented that at 7 weeks the medial geniculate body exhibited myelination, while at 9 weeks, both the auditory radiation and the splenium of the corpus callosum exhibited myelination. Yakovlev and Lecours [3] reported that the auditory radiation first showed myelination at 0 weeks, with the splenium of the corpus callosum showing myelination at 16 weeks. The MRI results indicate that the signal intensity changes occur much later than what has been reported for the histological research studies. A proposed explanation for this difference might be that it takes a minimal concentration of myelin to have a significant effect on the signal intensities during MR imaging, i.e., there must be a major

Table 1 Comparisons of histological and MRI studies

	MGB	AR	SC
Histological study			
Flechsig	7 weeks	9 weeks	9 weeks
Yakovlev, Lecours	–	0 weeks	16 weeks
MRI study (T = Tesla)			
Counsell (1.0 T)	28 fw	–	–
Nakagawa (1.5 T)	–	14–27 weeks (T1T2)	14–27 weeks (T1T2)
Bird (1.5 T)	–	–	40 weeks (T1T2)~
Our results (1.5 T)	10 weeks (T2)	19 (T1), 24 (T2) weeks	16 (T1), 24 (T2) weeks

MGB: medial geniculate body, AR: auditory radiation, SC: splenium of corpus callosum, fw: fetal weeks.
Counsell et al examined myelination-associated T2-weighted signal changes and determined that the medial geniculate body exhibited signal changes that were indicative of myelination at 28 fetal weeks, which is much earlier than what we found in the current study. Nakagawa et al. examined the auditory radiation and splenium of the corpus callosum and found signal changes for both areas at 54–67 gestational weeks (both T1- and T2-weighted). After converting gestational weeks to weeks after birth (gestational weeks minus 40 weeks), their results were similar to our results. Bird et al. examined the splenium of the corpus callosum and reported finding myelination at 10 months of age (40 weeks after birth).

change in the myelin sheath makeup such as the loss of water and the gain of lipids.

Our study indicated that in the medial geniculate body, significant myelination- associated intensity changes were identified in the T2-weighted images, although the T1-weighted images did show a slight change of intensity at an early time than was seen for the T2-weighted imaging. It has been reported that the T2-weighted sequences are superior to the T1-weighted sequences with regard to demonstrating the contrast between the gray matter nucleus and the surrounding white matter, and thus, are more suitable when evaluating the gray matter nucleus [28]. T2-weighted sequences were superior to T1-weighted sequences in demonstrating the contrast between gray matter nucleus (medial geniculate body) and surrounding white matter, therefore more suitable for evaluating gray matter nucleus. This finding agrees with our last paper results [1].

The reason for this might be because the T1-relaxation times for the gray matter nucleus and the white matter are not large enough in a high-field strength system to be detected [28]. In the deep gray matter nuclei, the T2-weighted MRI was superior at showing myelin while the T1-weighted MRI was better at showing myelin in the white matter tracts. This could be due to the characteristics of the anatomical area, as has been suggested in other MRI brain region studies [28,29]. Overall, these results suggest that fine-tuning of the protocols for the specific area to be examined may be useful when assessing myelination in brain.

4.2. Myelination progress from other aspects

For the visual system the duration of functional maturation (spatiotemporal vision) correlates with the duration of the myelination of the optic radiation [30–32]. Moore et al. [5] has postulated that the time of myelination onset in central auditory pathway coincides with the onset of the acoustico-motor reflexes or the auditory startle reaction. Therefore evaluating the myelination degree of the central auditory pathway would be needed for the research of hearing development in infants. However, as in this study we clarify the time lag between the histological study and MRI evaluation about normal myelination period, so comparing with histological work directly is not correct when evaluate the maturation of central auditory pathway using MRI. New milestone of central auditory pathway development using MRI is needed and we suggest this study results as new milestones. The current results which correlate with the auditory function would be useful for research of hearing development in infants using MRI.

5. Conclusion

Use of 1.5 T MRI to examine the central auditory nuclei and pathway of the higher brain revealed signal intensity changes associated with myelination that were approximately 3, 7–24, and 7–15 weeks after that reported in histological literature for the medial geniculate body, auditory radiation and splenium of the corpus callosum, respectively. The reason for the delay is considered to be related to the fact that myelination does not take place suddenly but rather, happens gradually over time. Thus, substantial changes of the myelin sheath makeup, a loss of water and the gain of lipids are required in order for the myelination to be detectable by MRI. This study also shows that MRI can be used to follow the myelination progress pattern in the central auditory pathway of the higher brain. In conjunction with our previous study on the auditory brainstem pathway, [1] these results indicate that MRI can be used to assess the maturation of the auditory system of infants.

Acknowledgements

This study was supported by a Grant-Aid for Young Scientists (B) from The Ministry of Education, Culture, Sports, Science and Technology (MEXT), Japan.

References

[1] M. Sano, K. Kaga, C.C. Kuan, K. Ino, K. Mima, Early myelination patterns in the brainstem auditory nuclei and pathway: MRI evaluation study, Int. J. Pediatr. Otorhinolaryngol. 71 (2007) 1105–1115.

[2] P. Flechsig, Anatomie des Menschichen Gehirn und Rueckenmarks auf Myelogenetischer Grundlage, Thime, Leipzig, 1920.

[3] P.I. Yakolvlev, A. Lecours, The myelogenetic cycles of regional maturation of the brain, in: A. Minkowski (Ed.), Regional Development of the Brain in Early Life, Blackwell Scientific Publication, Oxford, 1967, pp. 3–70.

[4] L.B. Rorke, H.E. Riggs, Myelination of the Brain in the Newborn, Lippincott Company, Philadelphia, 1969.

[5] J.K. Moore, L.M. Perazzo, A. Braun, Time course of axonal myelination in the human brainstem auditory pathway, Hear. Res. 87 (1/2) (1995) 21–31.

[6] H. Nakagawa, S. Iwasaki, K. Kichikawa, A. Fukusumi, T. Taoka, H. Ohishi, et al., Normal myelination of anatomic nerve fiber bundles: MR analysis, Am. J. Neuroradiol. 19 (1998) 1129–1136.

[7] M.A. Johnson, J.M. Pennock, G.M. Bydder, Clinical NMR imaging of the brain in children: normal and neurologic disease, AJR Am. J. Roentgenol. 141 (1983) 1005–1018.
[8] B.A. Holland, D.K. Haas, D. Norman, M. Brant-Zwadzki, T.H. Newton, MRI normal brain maturation, AJNR Am. J. Neuroradiol. 7 (1986) 201–208.
[9] R.B. Dietrich, W.G. Bradley Jr., MR evaluation of early myelination patterns in normal and developmentally delayed infants, AJNR 9 (1998) 69–76.
[10] C.B. McArdle, C.J. Richardson, D.A. Nicholas, M. Mirfakhraee, C.K. Hayden, E.G. Amparo, Developmental features of the neonatal brain: MR imaging, gray-white matter differentiation and myelination, Radiology 162 (1987) 223–229.
[11] M.S. van der Knaap, J. Valk, MR imaging of the various stage of normal myelination during the first year of life, Neuroradiology 31 (1990) 459–470.
[12] K. Hayakawa, Y. Konishi, M. Kuriyama, K. Konishi, T. Matsuda, Normal brain maturation in MRI, Eur. J. Radiol. 12 (1990) 208–215.
[13] E. Martin, R. Kikinis, M. Zuerrer, C. Boesch, J. Briner, G. Kewitz, et al., Development stages of human brain: an MR study, J. Comput. Assist. Tomogr. 12 (1988) 917–922.
[14] E. Martin, S. Krassnitzer, P. Kaelin, MR imaging of the brainstem: normal postnatal development, Neuroradiology 33 (1991) 391–395.
[15] A.J. Barkovich, B.O. Kjos, D.E. Jackson Jr., D. Norman, Normal maturation of the neonatal and infant brain: MR imaging at 1.5 T, Radiology 166 (1988) 173–180.
[16] C.R. Bird, M. Hedberg, B.P. Drayer, P.J. Keller, R.A. Flom, J.A. Hodak, MR assessment of myelination in infants and children: usefulness of marker sites, AJNR Am. J. Neuroradiol. 10 (1989) 731–740.
[17] J.A. Stone, D.W. Chakeres, P. Schmalbrock, High-resolution MR imaging of the auditory pathway, Magn. Reson. Imaging Clin. N. Am. 6 (1) (1998) 195–217.
[18] M.S. van der Knaap, J. Valk, MR imaging of the various stages of normal myelination during the first year of life, Neuroradiology 31 (1990) 459–470.
[19] D. Bergerbest, D.G. Ghahremani, D.E. Gabrieli, Neural correlates of auditory repetition priming: reduced fMRI activation in the auditory cortex, J. Cogn. Neurosci. 16 (2004) 966–977.
[20] K. Hittmair, D. Wimberger, T. Rand, L. Prayer, G. Bernert, J. Kramer, et al., MR assessment of brain maturation: comparison of sequences, AJNR 15 (1994) 425–433.
[21] B.D. Flannigan, W.G. Bradley Jr., J.C. Mazziotta, W. Rauschning, J.R. Bentson, R.B. Lufkin, et al., Magnetic resonance imaging of the brainstem: normal structure and basic functional anatomy, Radiology 154 (February (2)) (1985) 375–383.
[22] J.T. Curnes, P.C. Burger, W.T. Djang, O.B. Boyko, MR imaging of compact white matter pathways, AJNR Am. J. Neuroradiol. 9 (6) (1988) 1061–1068.
[23] A. Fee-Higins, J.C. Larroche, Development of the human Foetal Brain, INSERM Masson, Paris, 1987.
[24] Gaining and growing: Calculating corrected age, University of Washington's homepage, http://depts.washington.edu/growing/Assess/Grca.htm.
[25] T. Stricker, E. Martin, C. Boesch, Development of the human cerebellum observed with high-field-strength MR imaging, Radiology 177 (2) (1990) 431–435.
[26] W. Grodd, Normal and abnormal patterns of myelin development of the fetal and infantile human brain using magnetic resonance imaging, Curr. Opin. Neurol. Neurosurg. 6 (3) (1993) 393–397.
[27] M. Staudt, I. Krageloh-Mann, W. Grodd, Normal myelination in childhood brains using MRI—a meta analysis, Rofo 172 (10) (2000) 802–811.
[28] S.J. Counsell, E.F. Maalouf, A.M. Fletcher, P. Duggan, M. Battin, H.J. Lewis, et al., MR imaging assessment of myelination in the very preterm brain, AJNR Am. J. Neuroradiol. 23 (5) (May 2002) 872–881.
[29] A.J. Barkovich, Magnetic resonance techniques in the assessment of myelin and myelination, J. Inherit. Metab. Dis. 28 (3) (2005) 311–343.
[30] B.A. Brody, H.C. Kinny, A.S. Kloman, F.H. Gilles, Sequence of central nervous system myelination in human infancy, an autopsy study of myelination, J. Neuropathol. Exp. Neurol. 46 (1987) 283–301.
[31] H.C. Kinney, B.A. Brody, A.S. Kloman, F.H. Gilles, Sequence of central nervous system myelination in human infancy, patterns of myelination in autopsied infants, J. Neuropathol. Exp. Neurol. 47 (1988) 217–234.
[32] H.R. Wilson, Development of spatiotemporal mechanisms in infant vision, Vis. Res. 28 (1988) 611–628.

International Journal of Pediatric Otorhinolaryngology (2008) 72, 1751–1763

ELSEVIER

International Journal of Pediatric Otorhinolaryngology

www.elsevier.com/locate/ijporl

Myelination progression in language-correlated regions in brain of normal children determined by quantitative MRI assessment

Peijen Su [a], Chen-Chieh Kuan [a,*], Kimitaka Kaga [a], Masaki Sano [a], Kazuo Mima [b]

[a] *Department of Otorhinolaryngology and Head and Neck Surgery, Graduate School of Medicine and Faculty of Medicine, University of Tokyo, 7-3-1 Hongo, Bunkyo-ku, Tokyo 113-8655, Japan*
[b] *Division of Radiology, University of Tokyo Hospital, Tokyo, Japan*

Received 31 January 2008; received in revised form 14 May 2008; accepted 15 May 2008
Available online 11 October 2008

KEYWORDS
Myelination;
MRI study;
Language-correlated region;
Broca's area;
Wernicke's area;
Arcuate fasciculus;
Developing brain

Summary

Objective: To investigate the myelination progression course in language-correlated regions of children with normal brain development by quantitative magnetic resonance imaging (MRI) analysis compared with histological studies.
Methods: The subjects were 241 neurologically intact neonates, infants and young children (128 boys and 113 girls) who underwent MRI between 2001 and 2007 at the University of Tokyo Hospital, ranging in age from 0 to 429 weeks corrected by postnatal age. To compare their data with adult values, 25 adolescents and adults (14 men and 11 women, aged from 14 to 83 years) were examined as controls. Axial T2-weighted images were obtained using spin-echo sequences at 1.5 T. Subjects with a history of prematurity, birth asphyxia, low Apgar score, seizures, active systemic disease, congenital anomaly, delayed development, infarcts, hemorrhages, brain lesions, or central nervous system malformation were excluded from the analysis. Seven regions of interest in language-correlated areas, namely Broca's area, Wernicke's area, the arcuate fasciculus, and the angular gyrus, as well as their right hemisphere homologous regions, and the auditory cortex, the motor cortex, and the visual cortex were examined. Signal intensity obtained by a region-of-interest methodology progresses from hyper- to hypointensity during myelination. We chose the inferior cerebellar peduncle as the internal standard of maturation.
Results: Myelination in all these seven language-correlated regions examined in this study shared the same curve pattern: no myelination was observed at birth, it reached maturation at about 1.5 years of age, and it continued to progress slowly thereafter into adult life. On the basis of scatter plot results, we put these areas into three

* Corresponding author. Tel.: +81 3 5800 8665; fax: +81 3 3814 9486.
E-mail address: peijensu-tky@umin.ac.jp (C.-C. Kuan).

0165-5876/$ – see front matter
doi:10.1016/j.ijporl.2008.05.017

groups: Group A, which included the motor cortex, the auditory cortex, and the visual cortex, myelinated faster than Group B, which included Broca's area, Wernicke's area, and the angular gyrus before 1.5 years old; Group C, consisting of the arcuate fasciculus, has similar degree of myelination as Group B before 1.5 years but then myelinated more slowly after 3 years of age. No gender or left-right differences between homologous regions were found.

Conclusions: In this study, we determined the sequence of myelination of language-correlated regions in infants and children by quantitative MRI assessment. The higher cortical areas matured later than the primary cortical areas, and the arcuate fasciculus matured last. The observation that myelination reaches maturity after 18 months suggests that myelination may be a reason for the acceleration in vocabulary acquisition observed in children from that age. The slow pace of myelination also suggested the possibility of language development's continuation into early adult life. Myelination assessed by MRI was at least 1 month behind that assessed by histological staining. No gender or left-right hemisphere differences in myelination were noted.

1. Introduction

Language is a uniquely complex cognitive ability. Linguistic competence, which develops rapidly during early childhood, requires the cooperation among several areas of the cortex. An auditory signal received by the auditory cortex is understood after being processed in Wernicke's area, and then transmitted from Wernicke's area through the arcuate fasciculus to Broca's area. Broca's area, which performs the operation of verbalizing a message, then supplies it to the motor cortex, which drives the muscles used for speaking. When the subject is reading, the signal is received by the primary visual cortex and is delivered to the angular gyrus, which links the visual form of the written word with the corresponding auditory pattern in Wernicke's area. Speaking involves the same systems, but in a different order of operations.

It is well known that speech function is usually lateralized in the left hemisphere and hemispheric anatomical asymmetry is present at birth [1]. Maturation of the developing brain progresses rapidly in the early years and involves many changes in neuronal elements, including myelination [2] and synaptic pruning [3].

Myelination is an important process for brain development because it enhances the speed of neural communication and represents progression in functional brain maturation [4–7]. The maturation of myelination is virtually complete at the end of the first 2 years of life [7–9]. Nonetheless, myelination continues through childhood and into adulthood [10–12].

Before the development of magnetic resonance imaging (MRI), myelination was conventionally evaluated by histological staining methods [4,5,13,14]. Myelin is hydrophobic, and myelin formation is associated with a decrease in water content, which can be detected by MRI. The use of MRI to evaluate myelination visually and quantitative assessment of myelination-associated changes in the signal intensity of regions of interest (ROI) in the brain for detecting subtler changes has been reported [15–29]. However, a time lag has been noted between the determination of myelination by histological staining and its determination by MRI [7,15,21,29–31].

To date, there have been no studies specifically assessing the course of myelination in language-correlated regions of normal children by quantitative MRI assessment. The purpose of this study is to establish the progression of myelination in Broca's area, Wernicke's area, the arcuate fasciculus, and the angular gyrus, as well as their right hemisphere homologous regions, and the auditory cortex, the motor cortex, and the visual cortex in a normal developing brain.

1.1. Subjects

The subjects were 241 neurologically intact neonates, infants and young children (128 boys and 113 girls) who underwent MRI between 2001 and 2007 at the University of Tokyo Hospital, ranging in age from 0 to 429 weeks (8 years 3 months) by corrected postnatal age. For comparison with adult values, 25 adolescents and adults (14 men and 11 women, aged from 14 to 83 years) were examined as the control. These patients underwent MRI because a brain disorder was suspected: subjects with a history of prematurity, birth asphyxia, low Apgar score, seizures, active systemic disease, congenital anomaly, delayed development, infarcts, hemorrhages, brain lesions, or central nervous system malformation were excluded from analysis. The study protocol

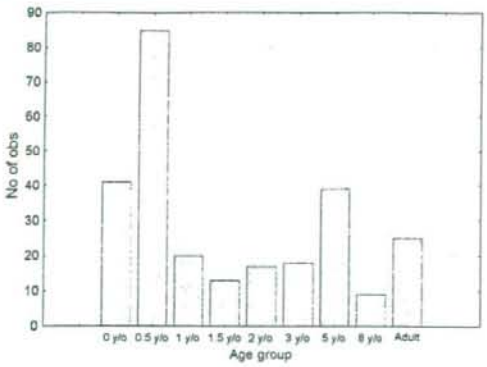

Fig. 1 Age distribution of the study population.

was approved by the Ethics Committee of the University of Tokyo. The corrected postnatal week (CPW) was calculated in accordance with the definition established by the World Health Organization, that is, by subtracting the number of weeks a child was born prematurely from the current age in weeks [32]. The age distribution of subjects is shown in Fig. 1.

1.2. Imaging methods

Axial T2-weighted magnetic resonance (MR) images were obtained using spin-echo sequences at 1.5 T (MagnetomVision 1.5 T, Siemens, Germany, Signa Excite HD 1.5 T, GE, USA). Sections were perpendicular to the long axis of the brain and 5–7 mm thick. Repetition time (TR) and echo time (TE) in T2-weighted images were 3000 ms and 70–100 ms, respectively. On the basis of previous studies, T2-weighted images were used because they correlate well with myelin-containing macroslices of age-matched postmortem brains and, they yield better gray and white matter contrasts than T1-sequences, and are therefore more suitable for evaluating maturation [23,24]. On T2-weighted MR images, signal intensity obtained by a region-of-interest method progresses from hyper- to hypointensity during myelination.

1.3. Depiction of regions of interest

For quantitative analysis, signal intensity was measured by the region-of-interest (ROI) method. Values for each ROI were determined using Centricity Web-J software (GE Yokogawa Medical Systems, Inc., Tachikawa, Japan). Seven regions of interest (ROIs) in language-correlated regions, namely Broca's area, Wernicke's area, the arcuate fasciculus, the angular gyrus, and their homologous regions in the right hemisphere as well as the auditory cortex,

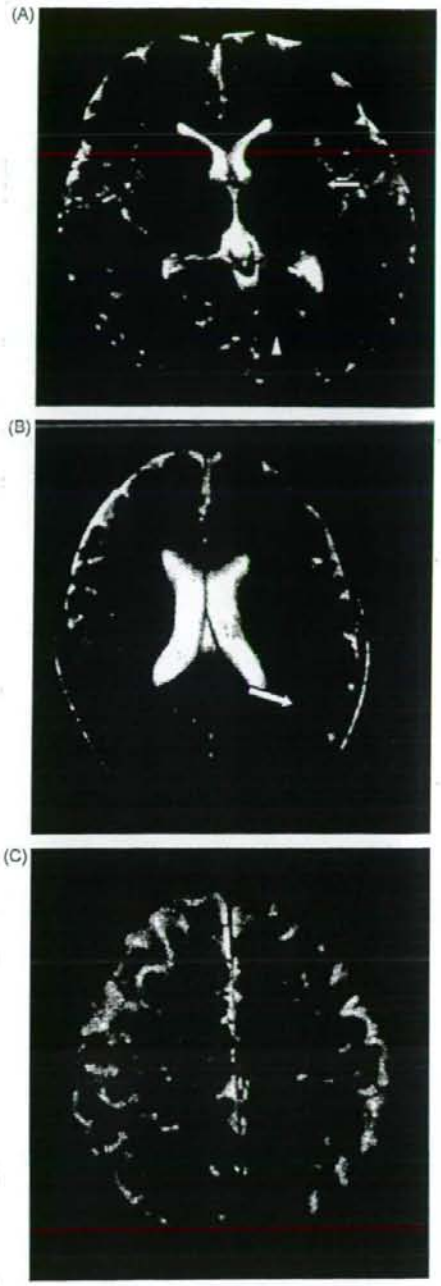

Fig. 2 (A) Depiction of regions of interest (T2-weighted images). Black arrow indicates Broca's area; white arrow indicates arcuate fasciculus; black arrowhead indicates auditory cortex; white arrowhead indicates visual cortex. (B) Black arrow indicates Wernicke's area; white arrow indicates angular gyrus. (C) Arrow indicates motor cortex.

the motor cortex, and the visual cortex were evaluated. We measured the subcortical white matter of Broca's area, Wernicke's area, the angular gyrus, the auditory cortex, the motor cortex, and the visual cortex. The boundaries and locations of these ROIs were typically as demonstrated in Fig. 2. Each ROI is about 8 pixels (0.22 cm^2) sampled about 1 mm just below the crest of the gyri cortex. In this study, we chose the inferior cerebellar peduncle as the internal standard of maturation.

1.4. Location of ROI

1. Wernicke's area (sensory, Brodmann area 22) is located in the posterior part of the superior temporal gyrus and lies between the primary auditory cortex and the angular gyrus (Brodmann area 39).
2. An important part of Wernicke's area projects into the motor speech area, Broca's area, via a corticocortical association pathway called the arcuate fasciculus. The arcuate fasciculus runs between the temporal, parietal and frontal lobes, and conjoins Wernicke's area, the visual-auditory conversion language area, and Broca's area.
3. Broca's area (motor speech, Brodmann area 44) lies in the frontal lobe, anterior to the primary motor and premotor cortex, corresponding to cytoarchitectonic areas 44 and 45 of the inferior frontal gyrus.
4. The primary motor cortex (Brodmann area 4) is located in the dorsal part of the precentral gyrus and the anterior bank of the central sulcus.
5. The primary visual cortex can be recognized by Gennari's band located in the occipital lobe in the upper and lower lips of the calcarine sulcus.
6. The primary auditory cortex (Brodmann area 41) is located in the anterior transverse temporal gyrus (of Heschl) on the floor of the lateral sulcus and is surrounded by higher-order auditory cortical areas (cytoarchitectonic areas 42 and 22), located on both the superior and lateral surfaces of the temporal lobe in the superior temporal gyrus.
7. The visual-auditory conversion language area is located in the angular gyrus.

1.5. ROI-based analysis

Counts for each ROI were measured using Centricity Web-J software (GE Yokogawa Medical Systems, Inc., Tachikawa, Japan). The ROIs were carefully chosen to minimize the effect of partial volume averaging. The number of pixels within each ROI was recorded, with a minimum of five pixels for each ROI. The signal intensity ratio (SIR) was calculated using the ratio of the signal intensity of each of the designated areas of the brain to that of its ipsilateral vitreous body, which is in accordance with the method reported by McArdle [25], and also used by Abe [15].

$$SIR = \frac{S\,region}{S\,eyeball}$$

The vitreous body was chosen as the reference because its chemical composition and gel state remain constant during youth and young adulthood (perinatal to 30 years of age) [33–35].

1.6. Statistical analysis

In this study, statistical analysis was performed using SPSS software, Ver. 14.0 for Windows. The changes in the signal intensity ratio (SIR) in these ROIs were compared to the corrected postnatal week [32]. We analyzed the correlation between the signal intensity ratio (SIR) of each region and the subject's age. Multiple scatter plots and best-fit regression analyses were used to compare the myelination curves among the different regions in relation to the subject's age. One-way ANOVA with the Tukey–Kramer test was used for multiple comparisons among different age groups and for multiple SIR comparisons among different ROIs. We used the *t*-test with a box-and-whisker plot to compare, separately, ROIs in Group A (the motor cortex, visual cortex, and auditory cortex) with the ROIs in group B (Wernicke's area, Broca's area, and the angular gyrus) before 1.5 years of age, and to compare each ROI of group B with group C (the arcuate fasciculus) in the group from 3 to 8 years of age. We also used the *t*-test with a box-and-whisker plot to compare left-right hemisphere ROIs among different age groups and male and female ROIs in the same region. A *P*-value less than 0.05 denoted the presence of a significant difference.

2. Results

Age-related myelination progression was best-fitted with an exponential curve showing the variations in myelination velocity throughout the studied period.

1. The SIR of the inferior cerebellar peduncle was between 0.5 and 0.4 at birth and varied subtly with corrected age (Fig. 3H).
2. From one-way ANOVA, we found that in nearly all language-correlated regions, myelination had reached quasi-maturity by the 18th month and then slowed down after that, but continuing into

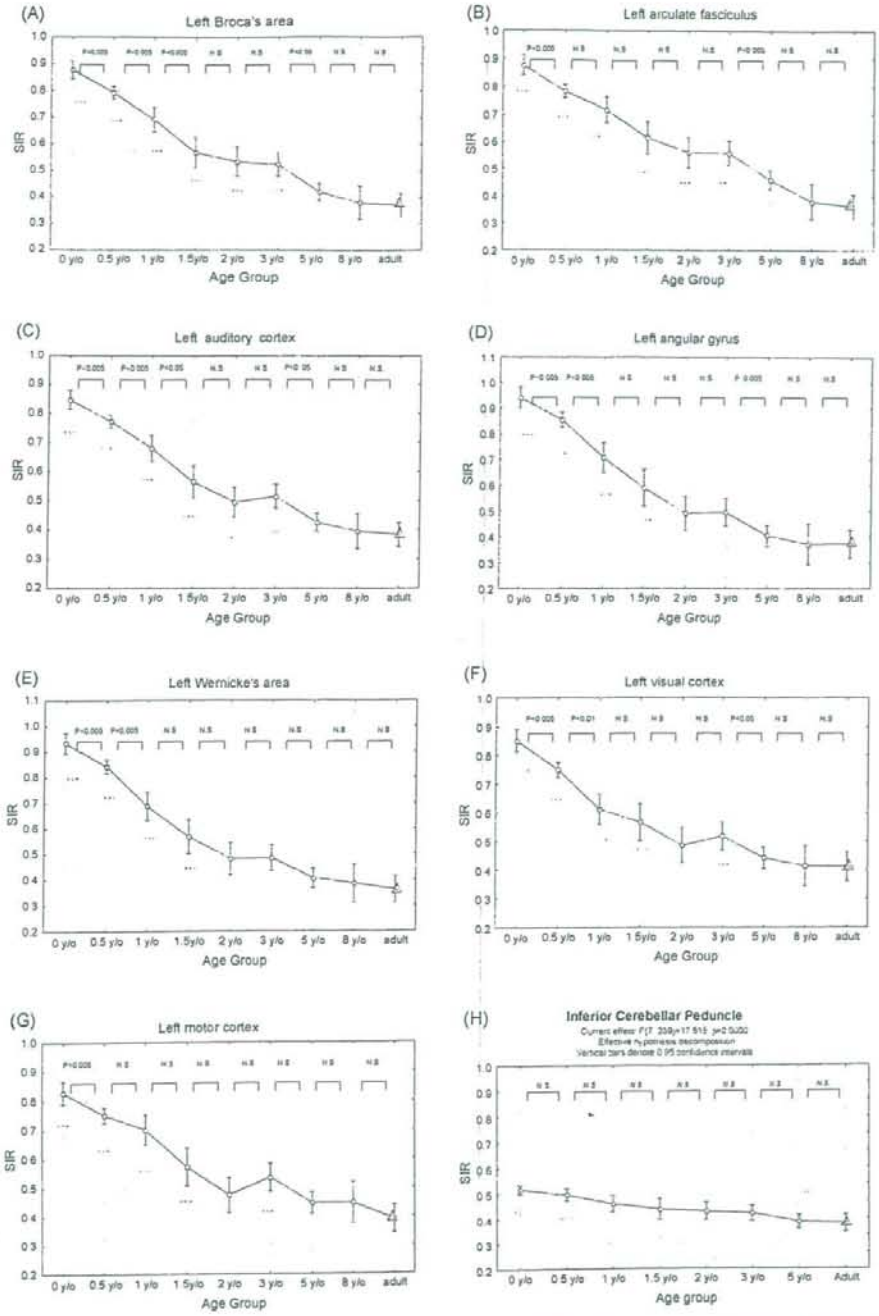

Fig. 3 The mean ± S.E.M. of the signal intensity ratio was obtained in different areas of the left hemisphere in each age group. N.S. not significant, $^{*}P < 0.05$, $^{**}P < 0.01$, $^{***}P < 0.005$. One-way ANOVA with the Tukey–Kramer test was used for multiple comparisons among different age groups. Red asterisks show the Tukey–Kramer multiple-comparison test with adult control group, marked by a red triangle. Vertical bars denote 0.95 confidence intervals. (The mean ± S.E.M. of the signal intensity ratio was also obtained in the same regions of the right hemisphere, which are not shown in this article.)

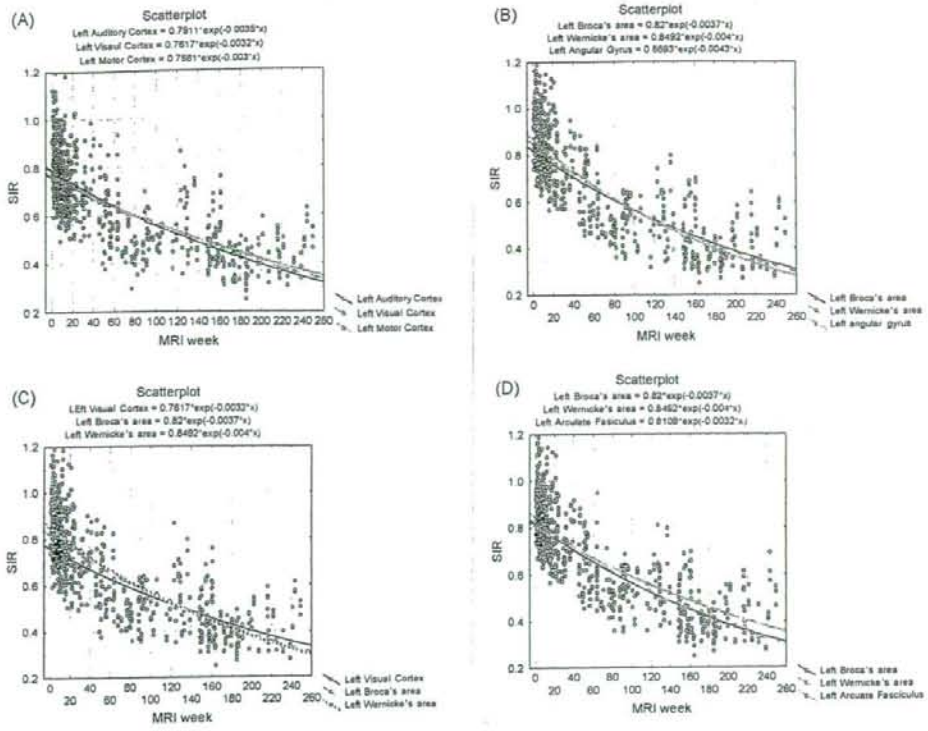

Fig. 4 Scatter plot graphs showing changes in the signal intensity ratio (SIR = *S* region/*S* eyeball) related to age. Each small circle is the SIR value in a given region for one subject at the time of measurement. The lines represent separate best-fit regression curves for each region. (A) Group A: Subjects' SIRs and best-fit regression curves for the left auditory cortex, the left visual cortex, and the left motor cortex. (B) Group B: Subjects' SIRs and best-fit regression curves for Wernicke's area, Broca's area, and angular gyrus. (C) Comparison between Group A and Group B. (C) Comparison between Group B and arcuate fasciculus.

adult life (Fig. 3A–G). Myelination shows similar patterns in these graphs. In the period from 0 to 1.5 years of age, the SIR changed from 0.88 to 0.5. In all regions, myelination continued progressively but slowly, the SIR reaching nearly 0.4 in the adult group. We further divided subjects aged younger than 6 months old into six groups at intervals of 1 month and carried out one-way ANOVA analysis. From the Tukey–Honestly Significant Differences (HSD) test, in Broca's area, Wernicke's area, the left arcuate fasciculus, the left visual cortex, the left motor cortex, and the left auditory cortex, the SIR showed a significant change from 4 months ($P < 0.05$), and in the left angular gyrus from 6 months ($P < 0.05$) (Fig. 7).

3. Based on the results of multiple scatter plots, we divided the regions under consideration into three groups. The motor cortex, auditory cortex, and visual cortex, which carry out primary functions, were classified into group A (Fig. 4A); Broca's area, Wernicke's area, and the angular gyrus, which are higher-order association areas, were classified into group B (Fig. 4B); and the arcuate fasciculus alone was classified into group C. From the *t*-test with a box-and-whisker plot, we found that myelination proceeded markedly faster in group A than in group B until 1.5 years of age ($P < 0.05$) (Fig. 4C); myelination of the arcuate fasciculus was similar to the pace of myelination in group B at the beginning of childhood but slower after 3 years of age (Fig. 4D).
4. When we analyzed the data using the *t*-test with a box-and-whisker plot, we found no gender difference (Fig. 5).
5. Likewise, we observed no left-right hemisphere differences between homologous regions (Fig. 6).

3. Discussion

No previous study has, to our knowledge, evaluated myelination specifically in language-correlated

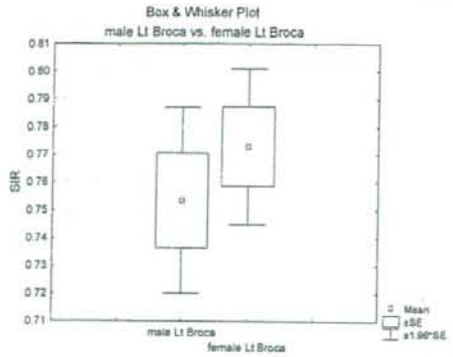

Fig. 5 Results of the *t*-test with a box and whisker plot comparing signal intensity ratio (SIR) differences (long axis) in Broca's area between male and female subjects in the age 0 group (shown in this figure) were not significant ($P = 0.384$). Other comparisons, which similarly failed to detect statistically significant sex differences in other ROIs, are not shown in this study.

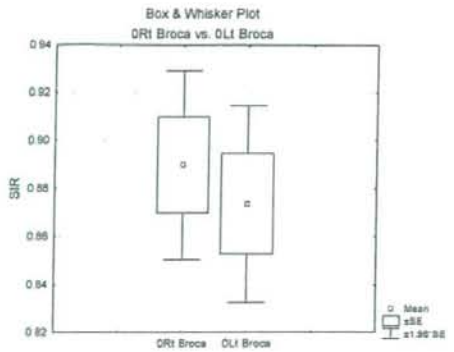

Fig. 6 Results of the *t*-test with a box and whisker plot comparing differences between Broca's area and the right hemisphere homolog of Broca's area in the age 0 group (shown in this figure) were not significant ($P = 0.57$). Other comparisons, which similarly failed to detect statistically significant hemisphere asymmetry in other age groups and in other ROIs, are not shown in this study.

regions of normal children. We therefore believe this to be the first study to have established the progression of myelination in Broca's area, Wernicke's area, and the arcuate fasciculus, the angular gyrus, the auditory cortex, the visual cortex, and the motor cortex in a normal developing brain by quantitative MRI assessment and to have compared the MRI with histological findings. This method is applicable clinically for the diagnosis of delayed myelination or demyelination. We compare our results with previous MRI studies and then with histological studies at the end of this paper.

3.1. Language processing

Language is an extremely complicated ability, involving several distinct areas of the cortex in order to complete linguistic processing. Linguistic competence requires coordination among these different areas of the cortex. Once an auditory signal has been detected, it is received by the auditory cortex, but it cannot be understood as a word until it has been processed in Wernicke's area. If a spoken word is heard, some representation is transmitted from Wernicke's area to Broca's area through a white fibrous tract called the arcuate fasciculus. Similar to a computer, Broca's area is responsible for the programming that verbalizes a message, which is then supplied to the face area of the motor cortex. The motor cortex then drives the muscles of the lips, the tongue, the larynx, etc., which are responsible for respiration, phonation, resonation, and articulation. When a written word is read, it is received by the primary visual cortex, then delivered to the angular gyrus, which joins the visual form of the word with the corresponding auditory pattern in Wernicke's area. Speaking the word involves the same neuronal systems mentioned above.

Generally speaking, Broca's area and Wernicke's area are the areas specifically responsible for the production and comprehension of language. The angular gyrus mediates between the visual and auditory forms of information, called the visual-auditory conversion language area. These specializations have only been detected on the left side. The corresponding areas on the contralateral side do not have the same linguistic ability.

The auditory sector of the language system, which comprises the pathway from the inner ear over the inferior colliculus to the auditory cortex, is functional prenatally from 20 to 24 gestational weeks (GW) of age [2]. The speech function is lateralized in the left hemisphere, and hemispheric anatomical asymmetry is present at birth. The language-mediating area of the superior surface of the temporal lobe (planum teporale), which is a part of the classical area of Wernicke, has been found to be statistically significantly larger on the left side both in neonates and adults [1,36]. Morphological asymmetry of the frontal operculum and temporal planum becomes measurable at the 29th GW [37].

3.2. Myelination examination by MRI

Language development during childhood is rapid, and maturation of the developing brain also progresses rapidly in the early years and involves many changes in neuronal elements, including

myelination [2], synaptic pruning [3], synaptogenesis, and dendritric and axonal arborization [6].

Myelination is the development of a protective myelin sheath around cranial nerves that facilitates neural functioning. It has been proven to be an important factor for brain maturation because it increases the propagation of neural impulses through the nerve system. The speed of neural transmission depends on not only on the synapses, but also structures of connecting fibers, which include axonal diameter and myelin sheath thickness. Myelination is associated with changes in water content owing to the expression of proteins and phospholipids. Because myelin is hydrophobic, composed of a bilayer of lipids with several large proteins, myelin formation is associated with a decrease in water content [8]. Myelination begins in the brain stem during the intrauterine stage, that is, 29 weeks [33], changes most rapidly during the first 2 years of life, and then continues throughout life.

Myelination proceeds from the inferior to superior, posterior to anterior, at different rates in different neuronal systems and in different tracts of the same neuronal systems [38]. Proximal pathways tend to myelinate before distal pathways, sensory areas before motor areas, and projection fibers before association fibers.

Histological studies of myelination have been reported previously [4,5,13,14]. However, it is difficult to evaluate the progression course of myelination owing to the scarcity of brain specimens. Therefore, the unique sensitivity of MRI to detect changes in water content offers opportunities to investigate the developmental process in vivo. However, a minimal threshold concentration of myelin build-up is necessary to change the signal intensity on MRI; thus, the MRI lags several weeks behind the histological timetable [7,15,21,29–31].

In previous studies, myelination was examined by using MRI qualitative or semiquantitative ratings in normal infants and children [8,15,16,18,20,22,27–30,36,38,39]. As many studies have shown that delayed myelination in children is related to developmental delay [13,14,16,31,40], it is important to establish the pace of myelination in normal children.

3.3. Previous MRI studies of myelination

Myelination during subcortical white matter maturation has been previously studied by T2-weighted MRI. Baierl et al. [16] mentioned that the subcortical white matter underwent a slow myelination. The contrast between gray and white matter continues to increase up to age 10 years whereas a rapid myelination of the internal capsule has been observed only in the first 2 years of life.

Holland et al. [21] reported that the subcortical white matter can be distinguished from the cortical gray matter at about 4–6 months by MRI assessment. Myelination begins around 9 months. The subcortical occipital white matter at 3 years shows a similar myelination level to that of adults, whereas the subcortical frontal white matter matures at 5 years. Owing to further minor refinements, the cortical white matter does not reach maturity until early adolescence.

The results of Girard et al. [41] differ from ours, and the results of Holland et al., Baierl et al., and Girard et al. mentioned that cortical myelination was visible in the occipital and ascending frontal regions as early as the 15th day of life, temporal region myelination had occurred at the age of 3 months, and cortical frontal myelination occurred last. Cortical myelination progressed in a rostral direction gradually and from place to place, developed earlier than that of the corresponding tracts, and was not continuous with it. Cortical myelination was completed at 26 months old, whereas our results showed myelination continuing later into adult life. Dietrich et al. [20] mentioned that myelination occurred in the optic radiations (3 months), the anterior limb of the internal capsule extending to the precentral gyrus (6 months), the parietal and frontal white matter (8 months), and the white matter of the temporal lobes (1 year), and later in the subcortical fibers. Dietrich [19] also reported that myelination progressed in the parietal and frontal white matter (8 months) and then in the white matter of the temporal lobe (1 year). After 1 year, myelination extended more peripherally and further myelinated subcortical fibers were noted at 2 years of age. Bird et al. [39] mentioned that the superficial or subarcuate white matter in the cerebral lobes showed similar patterns to the deep white matter, that is, it showed a slow progression of myelination and reached the same level of maturity as the internal capsule at about 2 years of age. This time course corresponds closely to our observation. Barkovich [17] found that the subcortical white matter (excluding the calcarine and rolandic areas) mature last; myelination begins at 9–12 months of age in the occipital lobe, at 11–14 months in the frontal lobe and then in the temporal lobe. He defined the peritrigonal region as the terminal zone, owing to its persistent hypersensitivity observed in T2-weighted images, and described it as the last associative area to mature. With the exception of the terminal zone, the entire white matter should mature by the 2nd year of life. However, Parazzini et al. [26] redefined the terminal zones of myelina-